ELSEVIER

Contents lists available at ScienceDirect

#### Acta Biomaterialia

journal homepage: www.elsevier.com/locate/actbio



Full length article

## Aligned skeletal muscle assembly on a biofunctionalized plant leaf scaffold



Junsu Yun<sup>a</sup>, Samantha Robertson<sup>b</sup>, Chanul Kim<sup>c</sup>, Masatoshi Suzuki<sup>b,\*</sup>, William L. Murphy<sup>a,c,d,\*</sup>, Padma Gopalan<sup>a,e,\*</sup>

- <sup>a</sup> Department of Materials Science and Engineering, University of Wisconsin-Madison, Madison, WI 53705, United States
- <sup>b</sup> Department of Comparative Biosciences, University of Wisconsin-Madison, Madison, WI 53705, United States
- <sup>c</sup> Department of Biomedical Engineering, University of Wisconsin-Madison, Madison, WI 53075, United States
- d Department of Orthopedics and Rehabilitation, University of Wisconsin School of Medicine and Public Health, Madison, WI 53705, United States
- <sup>e</sup> Department of Chemistry, University of Wisconsin-Madison, Madison, WI 53075, United States

#### ARTICLE INFO

# Article history: Received 17 March 2023 Revised 7 August 2023 Accepted 11 September 2023 Available online 18 September 2023

Keywords: Decellularized plant scaffold Parallel topography Polymer coating Human skeletal muscle cells

#### ABSTRACT

Decellularized plant scaffolds have drawn attention as alternative tissue culture platforms due to their wide accessibility, biocompatibility, and diversity of innate microstructures. Particularly, in this work, monocot leaves with innate uniaxial micropatterned topography were utilized to promote cell alignment and elongation. The leaf scaffold was biofunctionalized with poly(PEGMEMA-r-VDM-r-GMA) copolymer that prevented non-specific protein adsorption and was modified with cell adhesive RGD peptide to enable cell adhesion and growth in serum-free media. The biofunctionalized leaf supported the adhesion, growth, and alignment of various human cells including embryonic stem cells (hESC) derived muscle cells. The hESC-derived myogenic progenitor cells cultured on the biofunctionalized leaf scaffold adopted a parallel orientation and were elongated along the leaf topography. These cells showed significant early myogenic differentiation and muscle-like bundled myotube formation. The aligned cells formed compact myotube assemblies and showed uniaxial muscle contraction under chemical stimulation, a critical requirement for developing functional skeletal muscle tissue. Polymer-functionalized plant leaf scaffolds offer a novel human cell culture platform and have potential in human tissue engineering applications that require parallel alignment of cells.

#### Statement of significance

Plant scaffolds are plentiful sources in nature and present a prefabricated construct to present topographical cues to cells. Their feature width is ideal for human cell alignment and elongation, especially for muscle cells. However, plant scaffolds lack proteins that support mammalian cell culture. We have developed a polymer coated leaf scaffold that enables cell adhesion and growth in serum-free media. Human muscle cells cultured on the biofunctionalized leaf, aligned along the natural parallel micro-patterned leaf topography, and formed muscle-like bundled myotube assemblies. These assemblies showed uniaxial muscular contraction, a critical requirement for developing functional skeletal muscle tissue. The biodiversity of the plant materials offers a novel human cell culture platform with potential in human tissue engineering.

© 2023 Acta Materialia Inc. Published by Elsevier Ltd. All rights reserved.

#### 1. Introduction

Decellularized plant scaffolds have recently emerged as a new cell culture platform due to their unique attributes [1–4]. The de-

E-mail addresses: masatoshi.suzuki@wisc.edu (M. Suzuki), wlmurphy@ortho. wisc.edu (W.L. Murphy), pgopalan@wisc.edu (P. Gopalan).

cellularization process eliminates plant DNA and proteins from the tissue, while cell wall structure remains intact. The plant cell walls are composed of biocompatible materials such as cellulose, hemicellulose, and lignin, and include highly interconnected macroand micro-pores. A variety of plant species can provide different cell wall geometries, which can be useful for tissue engineering and biomedical applications. For example, decellularized bamboo stems were reported to have vertically oriented porous structures

<sup>\*</sup> Corresponding authors.

and were used to support the osteogenesis of mesenchymal stromal cells [5]. Decellularized vegetables and fruits (e.g., carrots, apples) with circular pores of varied sizes were studied in bone, tendon, and skeletal muscle tissue engineering [2,6,7]. Plant leaves (e.g., spinach, parsley) have blood vessel-like branching vasculature and were explored in cardiac, bone, and vascular tissue engineering [4,8,9]. Taken together, these studies have demonstrated that decellularized plant scaffolds are cost-effective, sustainable, and biocompatible, and they have advantages over animal-derived biomaterials. The mechanical property of the decellularized plant scaffold is another important aspect that must be considered for their use in regenerative medicine, however, studies to this effect are sparse. Our earlier study reported that decellularized spinach leaves have a maximum tangent modulus of 0.3 MPa, whereas the measured tensile strength and toughness of the decellularized sorghum leaves are 0.27 MPa and 5.93 kPa, respectively [4]. Though mechanical strength of the leaf materials decreases after decellularization, these values are well within the range of normal decellularized human cardiac tissue (0.2 - 0.5 MPa).

The structure presented by biomaterials can regulate cell behaviors. Specifically, parallelly patterned constructs such as micro/nano-grooves [10,11], wrinkles [12,13], and fibrils [14,15], can give contact guidance to cells, which can promote the alignment of cells along the patterns [16,17]. Micropatterned substrates have been fabricated by various methods such as photolithography [18], microfluidics [19], electrospinning [20], and 3D printing [21]. In contrast, plant scaffolds are plentiful sources in nature and can provide a prefabricated construct to present topographical cues to cells. Specifically, monocot leaves have narrow and long leaf shapes with parallel micro-patterned topography in the range of 10 - 50 µm created by epithelial cell walls [22]. This feature width is ideal for human cell alignment and elongation, especially for muscle cells that have hierarchical structures with highly aligned myofibrils [23-25]. Some of the recent reports used decellularized monocot plant scaffolds such as green onion [2], grass [26], and leek [27] to study cell alignment. They cultured and differentiated muscle cells using mouse or human myoblasts on non-functionalized or animal-derived proteins functionalized plant scaffolds.

One major limitation of decellularized plants is the lack of proteins that support mammalian cell attachment, growth, and proliferation. Therefore, the plant scaffold needs to be functionalized for mammalian cell culture. Decellularized plants have been coated with ECM-derived proteins such as collagen [28,29], gelatin [1,8], and fibronectin [2,4] to culture mammalian cells. However, ECM-derived biomaterials are animal-derived products which can suffer from high cost, batch-to-batch variations [30,31] and can induce antigenicity, immune response, and anaphylaxis in severe cases [32,33]. Synthetic coatings such as minerals [3], RGD-dopamine [3], and graphene oxide [27] have also been applied to promote cell attachment and growth. But these methods can change the innate structure of plants by blocking interconnected pores and diminishing topography due to the thick coating layer.

In this work, we develop a chemically defined plant leaf scaffold to culture human skeletal muscle cells. We chose sorghum leaves because their relatively large (5 – 10 cm wide and 50 cm long) leaves provide sufficient surface area to access a large number of samples and have less hairy trichomes that may interfere with cell culture. The ~25 μm microgrooves in sorghum leaves are also a good fit for the target cell types. To avoid the issues with using animal-derived materials and preserve inherent plant structure, we apply a previously reported [34–38] poly(poly(ethylene glycol) methyl ether methacrylate-ran-vinyl dimethyl azlactone-ranglycidyl methacrylate) (P(PEGMEMA-r-VDM-r-GMA), PVG) coating to the decellularized monocot leaves. In the PVG polymer, synthesized by reversible addition-fragmentation chain transfer polymerization, the PEGMEMA provides a cytophobic background, the

GMA cross-links the coating, and the VDM reacts efficiently with biomolecules via native chemical ligation chemistry [34]. The coating was modified with an integrin-binding cell adhesive peptide, RGD, to support adhesion and growth of cells [34–38]. This polymer-coated plant leaf maintained the leaf's intrinsic parallel micro-patterns. Human myogenic progenitor cells, which were derived from hESCs, were cultured on the chemically defined leaf scaffold. Our biofunctionalized leaf promoted cell alignment, differentiation, and maturation of the plated progenitors as functional human skeletal myotubes. Our study establishes a broadly applicable cell culture platform using the built-in framework of plant leaves and a synthetic biofunctionalizable polymer coating.

#### 2. Materials and methods

#### 2.1. Decellularization of plant leaf

Sorghum leaves (RTx430) were collected from the Wisconsin Crop Innovation Center at the College of Agricultural and Life Sciences, University of Wisconsin–Madison. The sorghum leaves (75 to 85-day-old) were rinsed with deionized water to remove dust and soil. About 300 pieces of leaves were punched out from 5 – 7 leaves into a round shape in 8- or 12-mm diameter and used for the following experiments. The leaves were treated in 5% sodium hydroxide (Fisher Scientific) for 24 h at room temperature. The leaves were then rinsed with deionized water for 30 min five times. Then, 50% bleach solution containing 4.13% sodium hypochlorite (Clorox, Oakland, CA) was added for one hour at room temperature until they were fully bleached and white-colored. The decellularized leaves (dLeaf) were rinsed with deionized water for 30 min five times. The leaves were freeze-dried and stored at room temperature or stored in ethanol at -20°C until usage.

#### 2.2. DNA and protein content quantification

Twenty dried native or decellularized leaf discs (12 mm diameter) were collected and their weights were measured. Then, they were ground by mortar and pestle. Fragments were resuspended in 1 mL of deionized water and then filtered through a 40 µm of cell strainer. DNA content was measured using a CyQUANT<sup>TM</sup> Cell Proliferation Assay kit (Invitrogen, Carlsbad, CA), and protein content was measured using Bradford reagent (Sigma Aldrich, St Louis, MA) with bovine serum albumin (BSA) standards. The amount of DNA and proteins was determined using a Victor3 spectrophotometer (Perkin Elmer, Waltham, MA) and normalized by the initial weight of each leaf.

#### 2.3. Synthesis of poly (PEGMEMA-r-VDM-r-GMA) copolymer

VDM monomer was synthesized in two steps followed the previous report by M.E. Levere et al. [39], and PVG copolymer was synthesized following the prior publication [34-38]. All materials were purchased from Sigma Aldrich if not stated separately. PEGMEMA (6.8 mmol, 2.04 g), VDM (2.5 mmol, 0.348 g), GMA (0.7 mmol, 0.1 g), and chain transfer agent, 2-cyano-2-propyl benzodithioate (0.01 mmol, 2.21 mg) were added to the flask with 13 mL of anisole. The mixture was degassed with three cycles of freeze-pump-thaw. Lastly, the initiator 2,2'-azobis(2methylpropionitrile) (0.01 mmol, 1.642 mg) was added, and polymerization proceeded at 70°C for 17 h. The solution was precipitated in hexane and then dissolved in tetrahydrofuran (THF) three times. The final solution had a light pink color and was stored in THF or ethanol at -20°C. The PVG copolymer was analyzed using gel permeation chromatography giving a Mn = 66,000 - 80,000 and dispersity of 2.21. Proton nuclear magnetic resonance spectroscopy data gave 59.5% of PEGMEMA, 27.7% of VDM, and 12.8% of

GMA composition. This composition provides the right balance of cytophobicity in the polymer to prevent non-specific adsorption of proteins, optimal crosslinking for film stability, and sufficient VDM units for peptide conjugation [34,35].

### 2.4. Poly-L-lysine, PVG copolymer coating, and peptide immobilization on the plant scaffold

The coating and the peptide immobilization process were stated in a prior publication [36-38]. dLeaf was rinsed with deionized water for 30 min three times. For the control experiment, glass coverslips (8 mm and 12 mm diameter) were rinsed with deionized water and ethanol for 10 min by sonication. dLeaf and glass coverslip were incubated in 0.1% (w/v) of poly-L-lysine (PLL) (MW 70,000-150,000) (Sigma Aldrich) for an hour at room temperature. The PLL coated dLeaf (PLL-dLeaf) or glass (PLL-Glass) was rinsed with deionized water and then ethanol three times, respectively. PVG polymer was coated by adding 0.5% (w/v) of PVG copolymer in ethanol to the PLL-dLeaf and the coverslips overnight at room temperature to allow crosslinking between primary amine groups in PLL and epoxy groups in PVG. The PVG coated dLeaf (PVG-dLeaf) and glass (PVG-Glass) were rinsed with ethanol and phosphate buffered saline (PBS) (pH 7.4) for 30 min twice. Peptide was immobilized on the PVG-dLeaf or PVG-Glass by adding 1 mM of peptides in PBS (CGGGRGDSP-am (RGD) or CGGGK\*(FITC)am) (GenScript) for 1.5 h at room temperature. The RGD modified dLeaf (RGD-dLeaf) and glass (RGD-Glass) were rinsed with PBS for 30 min twice and sterilized in 70% ethanol for 30 min before use.

#### 2.5. Plant leaf scaffold surface topography analysis

Surface topography of leaf samples was imaged by 3D optical profilometer (Zygo New view 9000) and scanning electron microscopy (SEM, Zeiss Leo 1550VP). For optical profilometer, 12 mm diameter leaf samples were prepared in water. Samples were placed on a glass slide and excess water was removed. The topographical feature width and height were defined as the x-distance between concaved patterns and the z-distance between the lowest and highest points. Sixty locations each from three samples were selected randomly and one-way ANOVA was performed for statistical analysis. For SEM measurement, leaf samples were dehydrated using standard protocol immersing sequentially in increasing concentrations of ethanol in water (25, 50, 75, and 95%), followed by increasing concentrations of hexamethyldisilazane (Sigma Aldrich) in ethanol (25, 50, 75, 95, and 100%) [40]. The samples were airdried overnight and then gold-sputtered for SEM imaging. Twentyfive locations each from three samples were selected randomly for measurement of widths using ImageJ software.

#### 2.6. Surface chemistry characterization

Leaf samples were analyzed by Attenuated total reflection Fourier-transform infrared spectroscopy (ATR-FTIR, Nicolet Magna 860 FT-IR) to evaluate chemical structures as well as polymer coating on the leaf scaffolds. Leaf samples (dLeaf, PLL-dLeaf, PVG-dLeaf, and RGD-dLeaf) were lyophilized before measurement. The surface of leaf scaffolds was analyzed with a resolution of 4 cm $^{-1}$  (n=10) and a range of 750 to 4000 cm $^{-1}$ .

#### 2.7. Cell culture and plating on biofunctionalized leaf scaffold

Human mesenchymal stromal cells (hMSC) (Lonza, Basel, Switzerland) were cultured in minimum essential medium- $\alpha$  ( $\alpha$ MEM) (Corning, Manassas, VA) with 10% fetal bovine serum (FBS) (Gibco, Dublin, Ireland) and 1% penicillin-streptomycin (PS), human umbilical vein endothelial cells (HUVEC) in Endothelial Cell

Growth Medium 2 (Promocell, Heidelberg, Germany), and dermal fibroblast (hDF) (ATCC, Manassas, VA) in Dulbecco's Modification of Eagle's Medium (DMEM) (Corning,) with 10% FBS and 1% PS. Cells were cultured in T75 flasks and passaged at 70-80% confluency using trypsin (Cytiva, Marlborough, MA) for 5 min, and used within 3 to 7 passages. To analyze cell adhesion on the leaf scaffolds, cells were stained with CellTracker<sup>TM</sup> Green (Invitrogen) at 37°C for 30 min. Then, 10,000 cells per leaf were seeded on the PVG-dLeaf and RGD-dLeaf and incubated at 37°C for 1 h. After incubation, the leaves with cells were rinsed with PBS to remove unattached cells. Remaining cells on the leaf scaffold (12 mm diameter) were imaged under a fluorescence microscope. The images of attached cells were adjusted by image-thresholding using ImageJ software, and the # and area of the cells were calculated and expressed as mean  $\pm$  standard deviation. Three replicates of each cell type were prepared. Statistical significance between PVG-dLeaf and RGD-dLeaf for each cell type was determined by Student's t-test.

Human myogenic progenitors were prepared from hESC as described previously [40–42]. Briefly, hESC colonies (WA09 line) were obtained from WiCell Research Institute (Madison, WI) and maintained by using a feeder-dependent culture protocol [43]. The colonies were lifted using 0.1% collagenase to form spherical aggregates named EZ spheres [40-42]. EZ spheres were maintained in the progenitor expansion medium [Stemline medium (Sigma Aldrich) supplemented with 100 ng mL<sup>-1</sup> recombinant human FGF-2 (WiCell), 100 ng mL<sup>-1</sup> human EGF (Millipore, Burlington MA), 5 ng m $L^{-1}$  heparin sulfate (Sigma Aldrich), and 1% penicillinstreptomycin-amphotericin (PSA) (ThermoFisher). Then, EZ spheres were passaged weekly by mechanical chopping using a McIlwain tissue chopper (Mickle Laboratory Engineering, Surrey, UK). After 6 weeks of culture, EZ sphere cells were dissociated by trypsin at 37°C for 5 min. Then, the dissociated cells (EZ H9) were seeded onto the substrates with a terminal differentiation medium (TDM, DMEM+GlutaMax with 2% B27 serum-free supplement and 1% PSA, all from ThermoFisher). For seeding cells, substrates were placed on a sterilized parafilm covered plate and cell solution was placed on the substrate in shape of hemispherical droplet. Cells were seeded with 3,000 cells cm<sup>-2</sup> on the RGD-dLeaf and with 2,000 cells cm<sup>-2</sup> on the RGD-Glass at 37°C for two hours. After two hours, the RGD-dLeaf and RGD-Glass substrates with cells were transferred to cell culture plates and kept cultured for up to 4 weeks. With 2,000 cells cm<sup>-1</sup> cell seeding density, RGD-dLeaf showed a lower cell number than RGD-glass, likely due to the increased surface area presented by the topography and intrinsic differences in material properties. As the initial cell density on the substrates is critical for myogenic differentiation, the cell seeding density was optimized to achieve the same cell confluency as RGD-Glass.

#### 2.8. Immunocytochemistry

Differentiated cells were fixed with ice-cold methanol for 10 min and blocked with 5% normal donkey serum (NDS) for 1 h. The cells were incubated with primary antibody (myosin heavy chain (MHC) or titin, 1:40 from Developmental Studies Hybridoma Bank (DSHB), Iowa City, IA) with 5% NDS for 1 h at room temperature or overnight at 4°C. Then, secondary antibodies conjugated to Cy3 or CF647 (1:1000) (Biotiom, Fremont, CA) with 5% NDS were stained for 30 min at room temperature. Cell nuclei were labeled with 0.5 mg mL<sup>-1</sup> of Hoechst 33258 nuclear dye in PBS (Sigma Aldrich). Plant cell nuclei were labeled with 5 mg mL<sup>-1</sup> of DAPI (ThermoFisher) in PBS overnight after fixation with 10% formalin. Images were acquired by using a fluorescence microscope. Orientation angle distribution and colorized map of MHC or titin-positive cells were measured by Image J software with the Orientation J plugin. Prior to analysis, the images of cells on RGD-dLeaf were

adjusted to the horizontal direction, but images of cells on RGD-Glass were analyzed as they are. The angle distributions of the RGD-dLeaf samples were fitted with Lorentzian distribution (data not shown) using Origin software, and three images of the entire substrate (12 mm diameter) were analyzed (n=3). Based on the fitted curve, the full width at half maximum (FWHM) and the angle at the center of peak were analyzed.

#### 2.9. Myotube contraction video analysis

Myotube contraction was analyzed as described in the previous study [42]. Myotubes on the leaf scaffolds were stained with 2 μM of Calcein-AM (Fisher Scientific) for 30 min at 37°C before taking video. Cells were stimulated by acetylcholine (Sigma Aldrich) in TDM with the final concentration at 0.1 – 1.0 mM. Upon stimulation, videos were taken using a Nikon Eclipse TS 100 inverted microscope with a QImaging camera (QImaging, Surrey, BC, Canada) and PCO Camera (PCO.panda 4.2 M, Wilmington, DE). The videos were recorded as AVI files by Q Capture Pro (QImaging) and NIS-Elements (Nikon) software. Image J was used to save individual frames as TIF files. Then, digital image correlation (DIC) was performed with Ncorr, an open-source Matlab software [44]. Displacement of subsequent images from a reference image was measured. The maximum displacement was analyzed from eight different locations per sample from three replicates.

#### 2.10. Statistical analysis

All experiments were performed with three replicates unless otherwise indicated, and data is expressed as means  $\pm$  standard deviations. For statistical analysis of data, Student's t-test or Oneway ANOVA was performed, and the statistical significance was considered at ns p > 0.05, \* p < 0.05, \*\* p < 0.01, and \*\*\* p < 0.001.

#### 3. Results

#### 3.1. Decellularization of leaf scaffold

Decellularization of plant leaf scaffold was carried out by alkali pretreatment and bleaching (Fig. 1A). Alkali pretreatment with 5% sodium hydroxide eliminates some plant cells, proteins, and waxy cuticles as well as gently oxidizes lignin and hemicellulose [45]. Plant leaves loose pigments during the alkali pretreatment as well (Fig. S1) [46]. This process enhances the efficiency of the bleaching process that removes the remaining plant cells and proteins. As a result of decellularization, both DNA and protein contents in the leaves dropped significantly (Fig. 1B). The amount of DNA reduced by approximately 9-fold (from 7.18  $\pm$  1.27 to 0.79  $\pm$  0.10  $\mu g$  mg $^{-1}$  Leaf) and protein decreased by 5-fold (from 27.11  $\pm$  3.75 to 5.60  $\pm$  0.07  $\mu g$  mg $^{-1}$  Leaf), which confirms effective decellularization. Direct staining of the nucleus with DAPI qualitatively shows the complete disappearance of cell nuclei in the decellularized leaf which supports the DNA analysis (Fig. S2).

#### 3.2. Biofunctionalization of decellularized leaf scaffold

The decellularized leaf was coated sequentially with PLL and PVG copolymer as described in previous studies because mammalian cells do not adhere to the leaves without further functionalization [36–38]. The positively charged PLL coats the dLeaf through electrostatic interactions with the slightly negatively charged leaf surface [47]. The PLL acts as an anchoring layer by covalently bonding with the PVG copolymer. The primary amines in PLL react with the epoxy ring of GMA units in PVG and crosslink the film. PVG-dLeaf was characterized by ATR-FTIR to confirm the

presence of PVG copolymer on the leaf scaffold (Fig. S3). Most peaks from dLeaf were similar to the IR spectrum reported for decellularized plants [5,9,27]. These peaks include the broad band at 3400 cm<sup>-1</sup> from O-H stretch, the 2917 and 2850 cm<sup>-1</sup> bands from C-H stretch, and the 1736 and 1650 cm<sup>-1</sup> from C=O stretch. These major peaks and others (1500 - 750 cm<sup>-1</sup>) represent the functional groups of cellulose, hemicellulose, and lignin, which are the three major components of plant scaffold [48,49]. The spectra of dLeaf, PLL-dLeaf, and PVG-dLeaf were mostly identical, except for a peak at 1818 cm<sup>-1</sup> detected in the PVG-dLeaf. This peak corresponds to the C=O stretch from the azlactone ester group in the PVG copolymer, confirming that the leaf scaffold was coated with PVG copolymer. After RGD peptide addition, the peak at 1818 cm<sup>-1</sup> decreases indicating successful conjugation of the RGD to the PVG coating. As the functionalization is limited to the surface, the residual 1818 cm<sup>-1</sup> signal may arise from the azlactone in the bulk of  $\sim$  4 nm thick PVG coating.

#### 3.3. Topography of the biofunctionalized leaf scaffold

Though the exact thickness could not be directly measured on the leaf scaffold, parallel studies on planar substrates show that PLL thickness is less than 4 nm, and a 4 - 10 nm PVG polymer coating on the PLL layer [37,50,51]. Thus, the polymer coating is on the nanometer scale and did not alter the leaf topography as confirmed by optical profilometer observations (Fig. 1C). Native leaves (nLeaf) have parallelly aligned topography with 25.65  $\pm$  5.04  $\mu m$ width (W) and microgrooves from the leaf epidermis that have a height (H) of 3.20  $\pm$  1.37  $\mu m$ . After decellularization and biofunctionalization, the W and H were preserved. The value of W and H for dLeaf was 25.44  $\pm$  7.01  $\mu$ m and 3.13  $\pm$  1.55  $\mu$ m respectively; for PVG-dLeaf 24.46  $\pm$  3.82 and 3.22  $\pm$  0.61  $\mu m$  respectively and for RGD-dLeaf 24.97  $\pm$  6.89  $\mu m$  and 3.18  $\pm$  1.36  $\mu m$  respectively. Additionally, the feature widths measured from SEM are also quite similar (Fig. S4). Hence, the polymer coating largely preserves the leaf topography.

#### 3.4. Human cell adhesion on the biofunctionalized leaf scaffold

Four different types of human cells, hDF, hMSC, and HUVEC (Fig. 1D), and hESC-derived myogenic progenitor cells (Fig. S5) were seeded onto the RGD-dLeaf scaffold, to evaluate the feasibility of culturing human cells. These cell types were chosen based on their common use in human cell culture and tissue engineering applications. PVG coating on the leaf prevented non-specific adsorption of proteins, hence all four cell types did not adhere to the PVG-dLeaf and showed a circular shape. On the other hand, the cells on the RGD-dLeaf showed polygonal morphologies after incubation for 1 h, indicating good attachment. The attached cell number and cell coverage on the RGD-dLeaf were also significantly higher than on PVG-dLeaf, which shows RGD peptide presence on the leaf surface. Also, the absence of adhesive cells on PVG-dLeaf and the full-coverage of cells on RGD-dLeaf indicate the homogeneity of the PVG coating (Fig. S6A). Upon culturing the cells for 7 days, the cells grew uniformly on the RGD-dLeaf. However, only the hESC-derived myogenic progenitor cells (Fig. S5D), hDFs (Fig. S6B), and hMSCs (Fig. S6C) aligned along the direction of leaf topography. Lack of alignment in 7-day cultured HUVEC (Fig. S6D) may be attributable to the nature of the ECM that is produced beyond 3 days of culture.

## 3.5. Muscle differentiation from human ESC-derived myogenic progenitor cells on the biofunctionalized leaf scaffold

Myogenic progenitor cells were plated on RGD-dLeaf and flat RGD-Glass (as control) and cultured for 3 weeks. The myogenic dif-

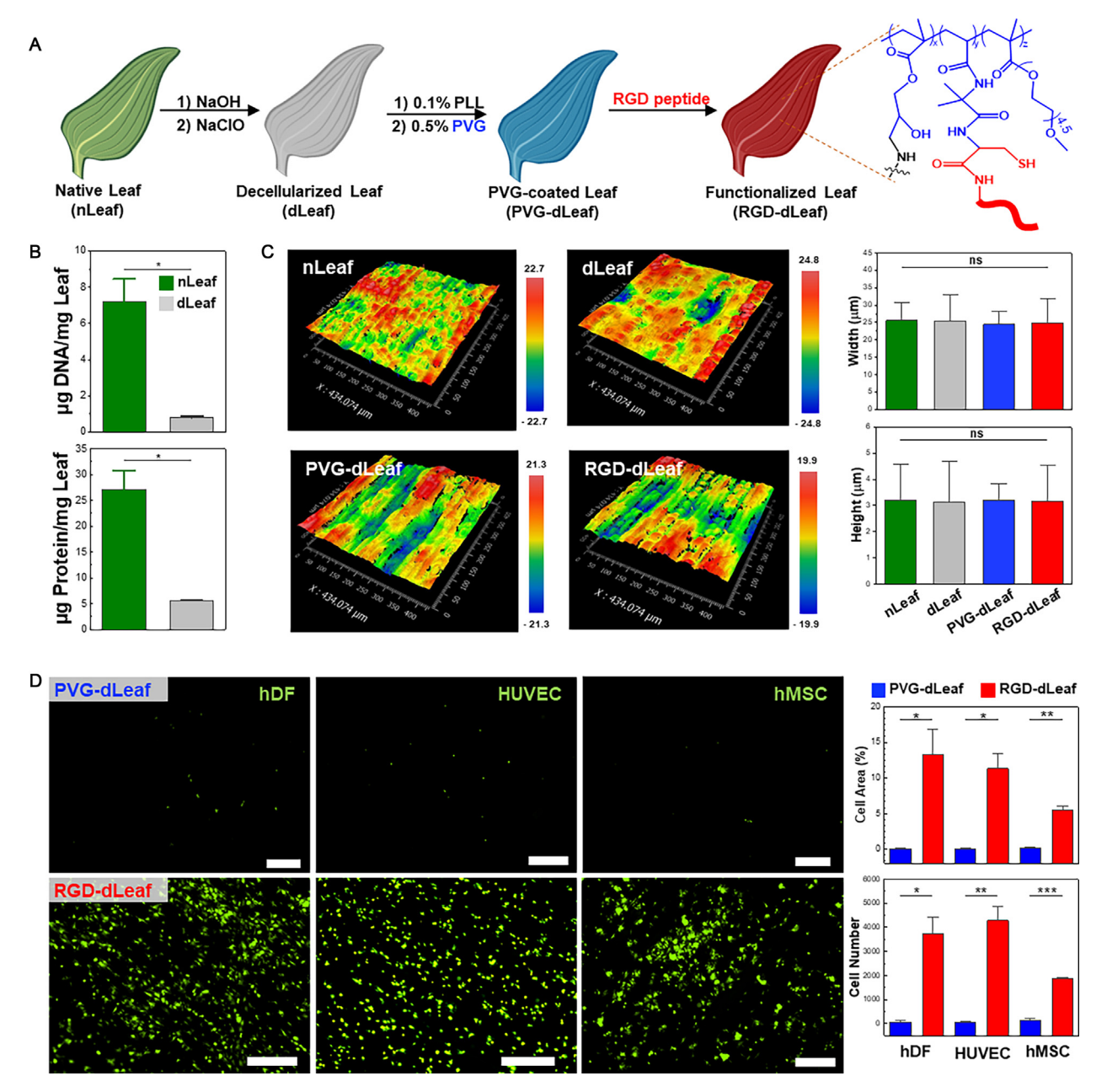


Fig. 1. Decellularization and biofunctionalization of sorghum leaf. (A) Scheme of decellularization and functionalization of leaf scaffolds, (B) DNA and protein contents of nLeaf and dLeaf. (C) Topography profile of nLeaf and RGD-dLeaf. (Unit:  $\mu$ m) (D) Adhesion of three types of human cells (hDF, hMSC, HUVEC) on the PVG-dLeaf and RGD-dLeaf after 1 hr culture. Scale bar: 500  $\mu$ m. ns p > 0.05, \* p < 0.05, \*\* p < 0.01, \*\*\* p < 0.001

ferentiation of the cells was assessed by immunocytochemistry using myosin heavy chain (MHC) and titin antibodies. After 7 days of differentiation, very few MHC+ cells were found, with some cells presenting multiple nuclei on the RGD-Glass (Fig. 2). In contrast, a greater number of MHC+ cells were found on the RGD-dLeaf. Many of the MHC+ myotubes on the RGD-dLeaf were multinucleated and elongated to a larger extent when compared to the cells seeded on the RGD-Glass. A qualitative comparison of the MHC+ cells on RGD-dLeaf clearly shows longer cells compared to those on RGD-Glass (Fig. S7). Similarly, the RGD-Glass contained a few titin<sup>+</sup> cells with striated sarcomeres after 7 days of differentiation (Figs. 2 and S8). In comparison, a greater number of titin+ cells with sarcomeres were found on the RGD-dLeaf. The presence of titin+ myotubes confirms sarcomere formation during differentiation [52,53]. Thus, the results of differentiation for 7 days indicate that the leaf topography promoted early myogenic differen-

tiation of the cells. After 10 days of differentiation, the cells on both RGD-Glass and RGD-dLeaf showed increased multinucleated MHC <sup>+</sup> cells, highly elongated myotubes, and clustering of cells as the number of myotubes increased. After 18 days of differentiation, myotubes on the RGD-dLeaf clustered forming muscle-like bundles parallel to the leaf topography over the entire leaf surface (Fig. S9). On the other hand, myotubes on the RGD-Glass showed bundled myotubes in random directions.

#### 3.6. Myotube orientation angle on the biofunctionalized leaf scaffold

The orientation angle of myotubes with respect to the leaf topography was measured and is shown using a color map (Figs. 3 and S10). The direction of the leaf topography was fixed as the horizontal direction (green lines). On RGD-Glass, the cells were elongated, forming locally aligned and clustered morphology with an

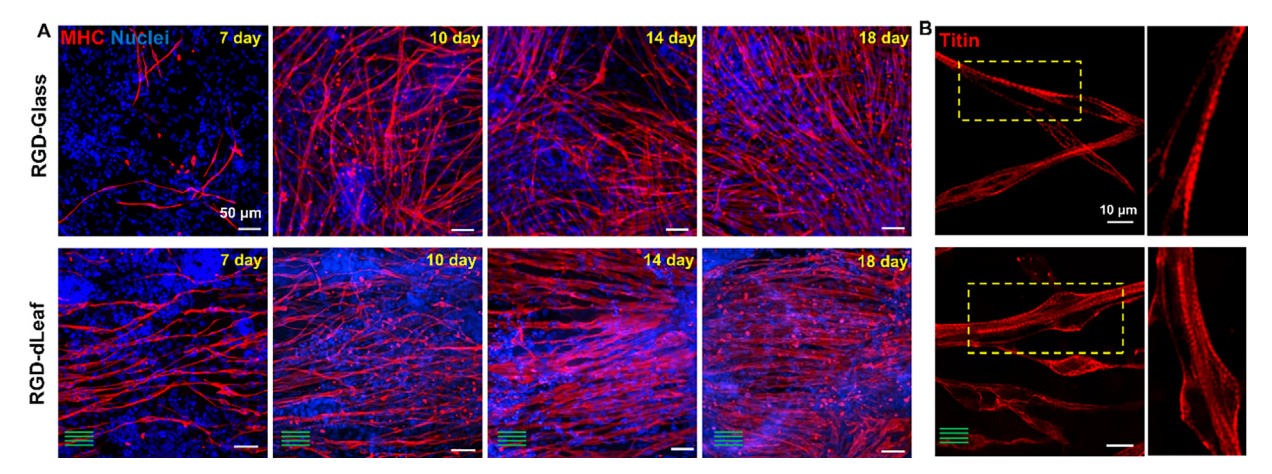


Fig. 2. Myogenic differentiation of ESC-derived muscle cells. Immunocytochemistry of (A) MHC and nuclei in differentiated cells for 7, 10, 14, and 18 days, and (B) titin at 7 days. Green bars show direction parallel to the leaf topography.

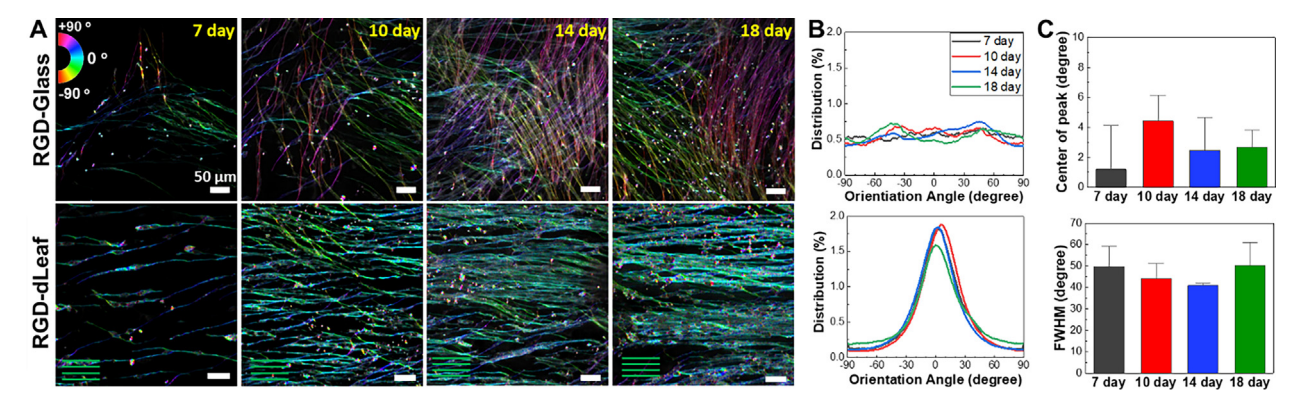


Fig. 3. Cellular alignment of differentiated cells (A) Representative color maps of MHC+ myotube orientation angle with respect to the leaf topography. Green bars show direction parallel to the leaf topography. (B) Orientation angle distribution of myotubes on the RGD-Glass (top) and RGD-dLeaf (bottom). (C) Center of peak (top) and full width at half maximum (bottom) of the orientation angle distribution of RGD-dLeaf.

overall random cell orientation after 14 days of differentiation. On the other hand, cells on RGD-dLeaf were aligned in the horizontal direction. The angles at the center of distribution were at 1.21  $\pm$  2.89°, 4.42  $\pm$  1.71°, 2.46  $\pm$  2.17°, and 2.68  $\pm$  1.15° and FWHM values were 49.73  $\pm$  9.42°, 44.17  $\pm$  7.01°, 40.93  $\pm$  1.15°, and 50.29  $\pm$  10.79° on day 7, 10, 14, and 18, respectively. Hence the orientation of cells in the horizontal direction was maximized at day 14 as the elongated myotubes got dense. But cells showed a marginally wider distribution in the orientation after day 18 due to the detachment of cells from the leaf surface (Fig. S10-4). These observations confirmed that the microgrooves on the leaf scaffold promoted parallel alignment and early myogenic differentiation of the myotubes and assembly of them into compact bundles.

#### 3.7. Myotube contraction by chemical stimulation

After 21 days of differentiation, myotubes were stimulated by acetylcholine and video recorded by live cell staining (Fig. 4A, Video S1 and S2). Myotubes on both RGD-Glass and RGD-dLeaf contracted within seconds of adding acetylcholine. Myotubes on the RGD-Glass showed contractions twice for 2 s per contraction and stopped responding thereafter (Video S1). On the other hand, myotubes on the RGD-dLeaf contracted every 1-2 s lasting for over a minute (Video S2). The contractions of myotubes were further analyzed by digital imaging correlation (DIC) using Ncorr, a software in MATLAB. Contraction that occurred along the leaf topography was marked as "horizontal" and perpendicular to the topography was marked as "vertical". The horizontal and vertical dis-

placement of myotubes from the original position was calculated in each frame and is shown in colored maps (Fig. 4B and Video S3). In the DIC results, the contractions on the RGD-Glass were non-directional with all (Video S3A and S3B), with nearly equal displaced in horizontal and vertical directions (Horizontal: 6.59  $\pm$  3.14  $\mu m$ , vertical: 5.93  $\pm$  6.45  $\mu m$ ) (Fig. 4C and 4D). In contrast, myotubes on the RGD-dLeaf showed contractions predominantly in the horizontal direction (Video S3C and S3D) (Horizontal: 6.56  $\pm$  2.63  $\mu m$ , vertical: 1.74  $\pm$  1.34  $\mu m$ ). The observed anisotropic contractions of the myotubes confirmed that the differentiated myotubes form functional muscle units.

#### 4. Discussion

Though decellularized plant scaffolds have unique properties that are useful as an alternative cell culture platform, they cannot support stable cell adhesion due to lack of mammalian cell proteins. Several studies have shown cell adhesion on unmodified decellularized plant scaffolds, likely mediated by the absorption of proteins derived from the serum [6,9,54]. Various proteins (e.g., fibronectin and collagen) have also been used to functionalize plant scaffolds [1,4,28,55]. However, animal-derived proteins may cause immunogenicity, and their compositions vary from batch-to-batch, potentially causing inconsistent results. More importantly, the interaction between the cell and the plant scaffold is not defined when it is mediated by absorbed proteins. In our work, myogenic cells were cultured in a serum-free medium, and the unmodified dLeaf did not support cell adhesion (Fig. S5). Thus, functionaliza-

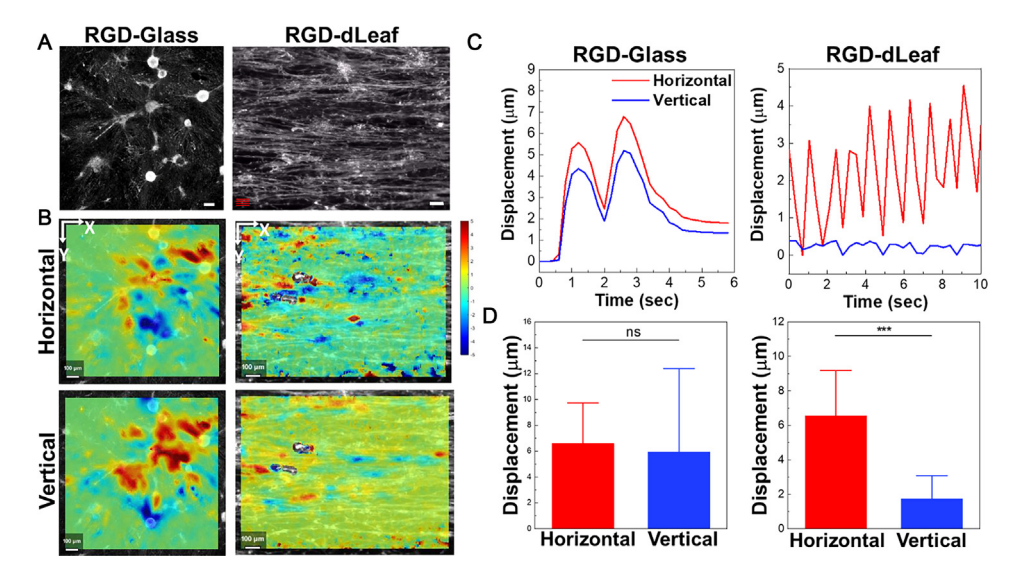


Fig. 4. Muscle contraction of differentiated myotubes by a chemical stimulus with acetylcholine. (A) Representative images of myotubes during contractions on RGD-Glass (left) and RGD-dLeaf (right) (scale bar: 100 μm). Red bars show direction parallel to the leaf topography. (B) Representative images of the myotube contraction analyzed by digital image correlation (DIC), (C) Displacements in the horizontal (red) and vertical (blue) directions during myotube contraction analyzed by DIC. (D) Maximum displacement of myotubes on RGD-Glass (left) and RGD-dLeaf (right) in the horizontal (red) and vertical (blue) directions. ns  $p \ge 0.05$ ; \*\*\* p < 0.001.

tion of decellularized plants is necessary to culture and grow cells in serum-free conditions. Our PVG coating provides a cytophobic background, and modification with an integrin-binding peptide, RGD, provides defined cell adhesion to the leaf scaffolds for over a month.

We have for the first time used sorghum leaves which are monocots with microgrooves  $\sim 25 \mu m$  to specifically culture hESCderived skeletal muscle cells. We also show their early myogenic differentiation to aligned myotubes, and uniaxial muscle contraction on these functionalized plant leaf scaffolds for the first time. The fact that we successfully demonstrate muscle contraction on these scaffolds shows that the polymer coating is also strengthening the decellularized leaf against tearing in addition to providing a defined platform for cell adhesion. The observation of anisotropic contraction in human myotubes is a crucial step toward developing functional muscle units with potential in clinical applications such as volumetric muscle loss injuries using human stem cell-derived muscle tissues. It is notable that recent reports have used decellularized plant scaffolds with W of 20-30 µm (onion leaf) [2], 100 µm (grass) [26], and 20 – 100  $\mu$ m (celery stalk) [54]. They studied myotube alignment and differentiation, limited to animal myoblast or primary human muscle cells, on either unfunctionalized plant scaffolds or on animal-derived protein functionalized scaffolds. None reported spontaneous muscle contraction in the myotubes.

The topography of plant leaf scaffold comes from the cell wall structure of the leaf epidermis which contains several types of epidermal cells such as guard, silica, trichome, and long pavement cells [56]. The long pavement epidermal cells mostly contribute to the parallel topography of the monocot leaf, while other cells are positioned in the interstitial space. Though cells other than pavement cells can influence cell alignment locally, they do not appear to interrupt the global alignment of myotubes in our work. The influence of the feature width on cell alignment has been studied before, where parallel microstructures with W ranging from 5 - 300 µm were fabricated for muscle cell culture [11,23,24]. They concluded that the 100 µm wide patterns did not promote significant cellular alignment because the patterns did not provide sufficient guidance to cells. In contrast, too narrow patterns (less than 5 μm) showed a lower differentiation fraction of myoblasts. The narrower patterns limited muscle cell density and direct cell-cell interactions which are required for membrane fusion and myogenic

differentiation [57]. The optimal alignment and differentiation results were found in 10 - 80 µm wide patterns. Notably, a variety of monocot plant species have 10 - 50 µm wide parallel microstructures [22]. The topography on the monocot sorghum leaf used in our study has a feature width of 25 µm, which is consistent with prior observations. Thus, decellularized plants can provide a variety of built-in microstructures with a broad range of biologically relevant feature sizes. Our studies have shown that the modification of PVG-coated leaf with global integrin-binding peptide, RGD, supports human cells' adhesion and myogenic cell differentiation of hESCs. In addition, the PVG coating can also be modified with other biomolecules to control surface biochemistry. Surface modification with ECM-mimic peptides has been reported to influence cell adhesion, proliferation, and differentiation. For example, a laminin-derived peptide, IKVAV, can promote muscle cell proliferation, migration, and fusions [58,59], and a collagen-derived peptide, DGEA, can regulate cell proliferation and differentiation [60,61]. Though our preliminary studies used only RGD to modify PVG coating, modification with such ECM-mimic peptides may induce different cellular responses. Hence, our polymer-coated plant leaf offers a generalizable cell culture platform with customizable surface chemistry and topography, for more defined and consistent cell culture platform, which is highly desirable for cell and tissue engineering studies.

#### 5. Conclusion

In summary, we demonstrated that the biofunctionalization of decellularized plant scaffolds can offer a novel platform for human cell culture, as their innate micropatterns can guide cell alignment. The decellularized plant leaf scaffolds were coated with a PVG polymer and modified with RGD peptide. The biofunctionalized leaf scaffolds supported human cell adhesion and growth while preserving their inherent microstructures. The micropatterns on the leaf scaffold supported the myogenic differentiation of hESCs forming highly aligned and assembled myotubes. Importantly, the assembled myotubes on the leaf scaffolds showed muscle contractions by chemical stimulation along the direction of the leaf topography, which is critical to developing functional muscle tissue. Overall, our studies demonstrate the first-time culture of hESC-

derived skeletal muscle cells using biofunctionalized plant scaffolds

#### **Declaration of Competing Interest**

The authors declare the following financial interests/personal relationships which may be considered as potential competing interests:

Padma Gopalan, William Murphy, Junsu Yun report financial support was provided by National Science Foundation. Masatoshi Suzuki reports financial support was provided by National Institutes of Health.

#### **CRediT authorship contribution statement**

Junsu Yun: Conceptualization, Methodology, Formal analysis, Investigation, Writing – original draft, Visualization. Samantha Robertson: Investigation, Resources. Chanul Kim: Investigation. Masatoshi Suzuki: Supervision, Resources, Writing – original draft. William L. Murphy: Supervision, Project administration, Funding acquisition, Writing – original draft. Padma Gopalan: Supervision, Project administration, Funding acquisition, Writing – original draft.

#### Acknowledgements

This research was funded by the National Science Foundation (NSF DMR# 2207275) for the development of polymer coating, plant scaffold, and cell studies, and by the National Institutes of Health R01AR077191, M.S., the Good Food Institute, the University of Wisconsin Foundation, and UW Stem Cell & Regenerative Medicine Center for the hESC-derived cell studies. The antibodies for myosin heavy chain (MF20) and Titin were obtained from the DSHB developed under the NICHD and maintained by the University of Iowa. The authors acknowledge support from staff and the use of equipment at the Materials Science Center at UW-Madison DMR-1121288 and DMR1720415. Schematic images created with BioRender.com.

#### Supplementary materials

Supplementary material associated with this article can be found, in the online version, at doi:10.1016/j.actbio.2023.09.016.

#### References

- [1] R.J. Hickey, D.J. Modulevsky, C.M. Cuerrier, A.E. Pelling, Customizing the shape and microenvironment biochemistry of biocompatible macroscopic plantderived cellulose scaffolds, ACS Biomater. Sci. Eng. 4 (11) (2018) 3726–3736.
- [2] Y.W. Cheng, D.J. Shiwarski, R.L. Ball, K.A. Whitehead, A.W. Feinberg, Engineering aligned skeletal muscle tissue using decellularized plant-derived scaffolds, ACS Biomater. Sci. Eng. 6 (5) (2020) 3046–3054.
- [3] G. Fontana, J. Gershlak, M. Adamski, J.S. Lee, S. Matsumoto, H.D. Le, B. Binder, J. Wirth, G. Gaudette, W.L. Murphy, Biofunctionalized plants as diverse biomaterials for human cell culture, Adv. Healthc. Mater. 6 (8) (2017) 1601225.
- [4] J.R. Gershlak, S. Hernandez, G. Fontana, L.R. Perreault, K.J. Hansen, S.A. Larson, B.Y. Binder, D.M. Dolivo, T. Yang, T. Dominko, M.W. Roll, P.J. Weathers, F. Medina-Bolivar, C.L. Cramer, W.L. Murphy, G.R. Gaudette, Crossing kingdoms: using decellularized plants as perfusable tissue engineering scaffolds, Biomaterials 125 (2017) 13–22.
- [5] C.C. Mohan, P. Unnikrishnan, A.G. Krishnan, M.B. Nair, Decellularization and oxidation process of bamboo stem enhance biodegradation and osteogenic differentiation, Mater. Sci. Eng. C 119 (2021) 111500.
- [6] J. Lee, H. Jung, N. Park, S.H. Park, J.H. Ju, Induced osteogenesis in plants decellularized scaffolds, Sci. Rep. 9 (1) (2019) 20194.
  [7] N. Contessi Negrini, N. Toffoletto, S. Farè, L. Altomare, Plant tissues as 3D nat-
- [7] N. Contessi Negrini, N. Toffoletto, S. Farè, L. Altomare, Plant tissues as 3D natural scaffolds for adipose, bone and tendon tissue regeneration, Front. Bioeng. Biotechnol. 8 (2020) 723.
- [8] S. Dikici, F. Claeyssens, S. MacNeil, Decellularised baby spinach leaves and their potential use in tissue engineering applications: studying and promoting neovascularisation, J. Biomater. Appl. 34 (4) (2019) 546–559.

- [9] A. Salehi, M.A. Mobarhan, J. Mohammadi, H. Shahsavarani, M.A. Shokrgozar, A. Alipour, Efficient mineralization and osteogenic gene overexpression of mesenchymal stem cells on decellularized spinach leaf scaffold, Gene 757 (2020) 144852.
- [10] X. Jiang, S. Takayama, X. Qian, E. Ostuni, H. Wu, N. Bowden, P. LeDuc, D.E. Ingber, G.M. Whitesides, Controlling mammalian cell spreading and cytoskeletal arrangement with conveniently fabricated continuous wavy features on poly (dimethylsiloxane), Langmuir 18 (8) (2002) 3273–3280.
- [11] S. Chen, T. Nakamoto, N. Kawazoe, G. Chen, Engineering multi-layered skeletal muscle tissue by using 3D microgrooved collagen scaffolds, Biomaterials 73 (2015) 23–31.
- [12] M. Guvendiren, J.A. Burdick, The control of stem cell morphology and differentiation by hydrogel surface wrinkles, Biomaterials 31 (25) (2010) 6511–6518.
- [13] A. Chen, D.K. Lieu, L. Freschauf, V. Lew, H. Sharma, J. Wang, D. Nguyen, I. Karakikes, R.J. Hajjar, A. Gopinathan, Shrink-film configurable multiscale wrinkles for functional alignment of human embryonic stem cells and their cardiac derivatives, Adv. Mater. 23 (48) (2011) 5785–5791.
- [14] J.S. Choi, S.J. Lee, G.J. Christ, A. Atala, J.J. Yoo, The influence of electrospun aligned poly (epsilon-caprolactone)/collagen nanofiber meshes on the formation of self-aligned skeletal muscle myotubes, Biomaterials 29 (19) (2008) 2899–2906.
- [15] H.G.Ş. Ayaz, A. Perets, H. Ayaz, K.D. Gilroy, M. Govindaraj, D. Brookstein, P.I. Lelkes, Textile-templated electrospun anisotropic scaffolds for regenerative cardiac tissue engineering, Biomaterials 35 (30) (2014) 8540–8552.
- [16] Y. Li, G. Huang, X. Zhang, L. Wang, Y. Du, T.J. Lu, F. Xu, Engineering cell alignment in vitro, Biotechnol. Adv. 32 (2) (2014) 347–365.
- [17] S. Wang, S. Hashemi, S. Stratton, T.L. Arinzeh, The effect of physical cues of biomaterial scaffolds on stem cell behavior, Adv. Healthc. Mater. 10 (3) (2021) 2001244.
- [18] P. Zorlutuna, N. Annabi, G. Camci-Unal, M. Nikkhah, J.M. Cha, J.W. Nichol, A. Manbachi, H. Bae, S. Chen, A. Khademhosseini, Microfabricated biomaterials for engineering 3D tissues, Adv. Mater. 24 (14) (2012) 1782–1804.
- [19] E. Kang, Y.Y. Choi, S.K. Chae, J.H. Moon, J.Y. Chang, S.H. Lee, Microfluidic spinning of flat alginate fibers with grooves for cell-aligning scaffolds, Adv. Mater. 24 (31) (2012) 4271–4277.
- [20] S.H. Ku, S.H. Lee, C.B. Park, Synergic effects of nanofiber alignment and electroactivity on myoblast differentiation, Biomaterials 33 (26) (2012) 6098–6104.
- [21] S.P. Pilipchuk, A. Monje, Y. Jiao, J. Hao, L. Kruger, C.L. Flanagan, S.J. Hollister, W.V. Giannobile, Integration of 3D printed and micropatterned polycaprolactone scaffolds for guidance of oriented collagenous tissue formation in vivo, Adv. Healthc. Mater. 5 (6) (2016) 676–687.
- [22] S. Bahadur, M. Ahmad, M. Zafar, S. Sultana, N. Begum, S. Ashfaq, S. Gul, M.S. Khan, S.N. Shah, F. Ullah, Palyno-anatomical studies of monocot taxa and its taxonomic implications using light and scanning electron microscopy, Microsc. Res. Tech. 82 (4) (2019) 373–393.
- [23] M.T. Lam, S. Sim, X. Zhu, S. Takayama, The effect of continuous wavy micropatterns on silicone substrates on the alignment of skeletal muscle myoblasts and myotubes, Biomaterials 27 (24) (2006) 4340–4347.
- [24] J.L. Charest, A.J. García, W.P. King, Myoblast alignment and differentiation on cell culture substrates with microscale topography and model chemistries, Biomaterials 28 (13) (2007) 2202–2210.
- [25] M.R. Salick, B.N. Napiwocki, J. Sha, G.T. Knight, S.A. Chindhy, T.J. Kamp, R.S. Ashton, W.C. Crone, Micropattern width dependent sarcomere development in human ESC-derived cardiomyocytes, Biomaterials 35 (15) (2014) 4454–4464.
- [26] S.J. Allan, M.J. Ellis, P.A. De Bank, Decellularized grass as a sustainable scaffold for skeletal muscle tissue engineering, J. Biomed. Mater. Res. Part A 109 (12) (2021) 2471–2482.
- [27] M. Toker, S. Rostami, M. Kesici, O. Gul, O. Kocaturk, S. Odabas, B. Garipcan, Decellularization and characterization of leek: a potential cellulose-based biomaterial, Cellulose 27 (13) (2020) 7331–7348.
- [28] J. Lacombe, A.F. Harris, R. Zenhausern, S. Karsunsky, F. Zenhausern, Plant-based scaffolds modify cellular response to drug and radiation exposure compared to standard cell culture models, Front. Bioeng. Biotechnol. 8 (2020) 932.
- [29] E.R. Robbins, G.D. Pins, M.A. Laflamme, G.R. Gaudette, Creation of a contractile biomaterial from a decellularized spinach leaf without ECM protein coating: an *in vitro* study, J. Biomed. Mater. Res. Part A 108 (10) (2020) 2123–2132.
- [30] X. Zheng, H. Baker, W.S. Hancock, F. Fawaz, M. McCaman, E. Pungor Jr, Proteomic analysis for the assessment of different lots of fetal bovine serum as a raw material for cell culture. Part IV. Application of proteomics to the manufacture of biological drugs, Biotechnol. Prog. 22 (5) (2006) 1294–1300.
- [31] C.W. Cheng, L.D. Solorio, E. Alsberg, Decellularized tissue and cell-derived extracellular matrices as scaffolds for orthopaedic tissue engineering, Biotechnol. Adv. 32 (2) (2014) 462–484.
- [32] A. Mackensen, R. Dräger, M. Schlesier, R. Mertelsmann, A. Lindemann, Presence of IgE antibodies to bovine serum albumin in a patient developing anaphylaxis after vaccination with human peptide-pulsed dendritic cells, Cancer Immunol. Immunother. 49 (3) (2000) 152–156.
- [33] J.L. Spees, C.A. Gregory, H. Singh, H.A. Tucker, A. Peister, P.J. Lynch, S.C. Hsu, J. Smith, D.J. Prockop, Internalized antigens must be removed to prepare hypoimmunogenic mesenchymal stem cells for cell and gene therapy, Mol. Ther. 9 (5) (2004) 747–756.
- [34] S.K. Schmitt, D.J. Trebatoski, J.D. Krutty, A.W. Xie, B. Rollins, W.L. Murphy, P. Gopalan, Peptide conjugation to a polymer coating via native chemical ligation of azlactones for cell culture, Biomacromolecules 17 (3) (2016) 1040–1047.

- [35] S.K. Schmitt, A.W. Xie, R.M. Ghassemi, D.J. Trebatoski, W.L. Murphy, P. Gopalan, Polyethylene glycol coatings on plastic substrates for chemically defined stem cell culture, Adv. Healthc. Mater. 4 (10) (2015) 1555–1564.
- [36] J.D. Krutty, A.D. Dias, J. Yun, W.L. Murphy, P. Gopalan, Synthetic, chemically defined polymer-coated microcarriers for the expansion of human mesenchymal stem cells, Macromol. Biosci. 19 (2) (2019) 1800299.
   [37] J.D. Krutty, J. Sun, K. Koesser, W.L. Murphy, P. Gopalan, Polymer-coated mag-
- [37] J.D. Krutty, J. Sun, K. Koesser, W.L. Murphy, P. Gopalan, Polymer-coated magnetic microspheres conjugated with growth factor receptor binding peptides enable cell sorting, ACS Biomater. Sci. Eng. 7 (12) (2021) 5927–5932.
   [38] J.D. Krutty, K. Koesser, S. Schwartz, J. Yun, W.L. Murphy, P. Gopalan, Xeno-free
- [38] J.D. Krutty, K. Koesser, S. Schwartz, J. Yun, W.L. Murphy, P. Gopalan, Xeno-free bioreactor culture of human mesenchymal stromal cells on chemically defined microcarriers, ACS Biomater. Sci. Eng. 7 (2) (2021) 617–625.
- [39] M.E. Levere, S. Pascual, L. Fontaine, Stable azlactone-functionalized nanoparticles prepared from thermoresponsive copolymers synthesized by RAFT polymerization, Polym. Chem. 2 (12) (2011) 2878–2887.
- [40] T. Hosoyama, J.V. McGivern, J.M. Van Dyke, A.D. Ebert, M. Suzuki, Derivation of myogenic progenitors directly from human pluripotent stem cells using a sphere-based culture, Stem Cells Transl. Med. 3 (5) (2014) 564–574.
- [41] S. Jiwlawat, E. Lynch, J. Glaser, I. Smit-Oistad, J. Jeffrey, J.M. Van Dyke, M. Suzuki, Differentiation and sarcomere formation in skeletal myocytes directly prepared from human induced pluripotent stem cells using a sphere-based culture, Differentiation 96 (2017) 70–81.
- [42] N. Jiwlawat, E.M. Lynch, B.N. Napiwocki, A. Stempien, R.S. Ashton, T.J. Kamp, W.C. Crone, M. Suzuki, Micropatterned substrates with physiological stiffness promote cell maturation and Pompe disease phenotype in human induced pluripotent stem cell-derived skeletal myocytes, Biotechnol. Bioeng. 116 (9) (2019) 2377–2392.
- [43] J.A. Thomson, J. Itskovitz-Eldor, S.S. Shapiro, M.A. Waknitz, J.J. Swiergiel, V.S. Marshall, J.M. Jones, Embryonic stem cell lines derived from human blastocysts, Science 282 (5391) (1998) 1145–1147.
- [44] J. Blaber, B. Adair, A. Antoniou, Ncorr: open-source 2D digital image correlation matlab software, Exp. Mech. 55 (6) (2015) 1105–1122.
- [45] K. Michalska, M. Bizukojć, S. Ledakowicz, Pretreatment of energy crops with sodium hydroxide and cellulolytic enzymes to increase biogas production, Biomass Bioenergy 80 (2015) 213–221.
- [46] C. Hawkins, D. Pattison, M. Davies, Hypochlorite-induced oxidation of amino acids, peptides and proteins, Amino Acids 25 (3) (2003) 259–274.
- [47] J. Budd, T.M. Herrington, Surface charge and surface area of cellulose fibres, Colloids Surf. 36 (3) (1989) 273–288.
- [48] K. Pandey, A. Pitman, FTIR studies of the changes in wood chemistry following decay by brown-rot and white-rot fungi, Int. Biodeterior. Biodegrad. 52 (3) (2003) 151–160.

- [49] M. Bergs, G. Völkering, T. Kraska, R. Pude, X.T. Do, P. Kusch, Y. Monakhova, C. Konow, M. Schulze, *Miscanthus x giganteus* stem versus leaf-derived lignins differing in monolignol ratio and linkage, Int. J. Mol. Sci. 20 (5) (2019) 1200.
- [50] D. Volodkin, H. Mohwald, J.C. Voegel, V. Ball, Coating of negatively charged liposomes by polylysine: drug release study, J. Control. Release 117 (1) (2007) 111–120.
- [51] L. Bużańska, A. Ruiz, M. Zychowicz, H. Rauscher, L. Ceriotti, F. Rossi, P. Colpo, K. Domańska-Janik, S. Coecke, Patterned growth and differentiation of human cord blood-derived neural stem cells on bio-functionalized surfaces, Acta Neurobiol. Exp. 69 (2009) 24–36.
- [52] P.F. van der Ven, G. Schaart, P.H. Jap, R.C. Sengers, A.M. Stadhouders, F. Ramaekers, Differentiation of human skeletal muscle cells in culture: maturation as indicated by titin and desmin striation, Cell Tissue Res. 270 (1) (1992) 189–198.
- [53] L. Tskhovrebova, J. Trinick, Titin: properties and family relationships, Nat. Rev. Mol. Cell Biol. 4 (9) (2003) 679–689.
- [54] S. Campuzano, N.B. Mogilever, A.E. Pelling, Decellularized plant-based scaffolds for guided alignment of myoblast cells, BioRxiv (2020).
- [55] D.J. Modulevsky, C. Lefebvre, K. Haase, Z. Al-Rekabi, A.E. Pelling, Apple derived cellulose scaffolds for 3D mammalian cell culture, PLoS ONE 9 (5) (2014) e97835.
- [56] R. Crang, S. Lyons-Sobaski, R. Wise, Plant Anatomy: A Concept-Based Approach to the Structure of Seed Plants, Springer, 2018.
- [57] J. Gurdon, E. Tiller, J. Roberts, K. Kato, A community effect in muscle development, Curr. Biol. 3 (1) (1993) 1–11.
- [58] K.I. Tashiro, G.C. Sephel, B. Weeks, M. Sasaki, G.R. Martin, H.K. Kleinman, Y. Yamada, A synthetic peptide containing the IKVAV sequence from the A chain of laminin mediates cell attachment, migration, and neurite outgrowth, J. Biol. Chem. 264 (27) (1989) 16174–16182.
- [59] C.E. Cimenci, G. Uzunalli, O. Uysal, F. Yergoz, E.K. Umay, M.O. Guler, A.B. Tekinay, Laminin mimetic peptide nanofibers regenerate acute muscle defect, Acta Biomater. 60 (2017) 190–200.
- [60] K.M. Hennessy, B.E. Pollot, W.C. Clem, M.C. Phipps, A.A. Sawyer, B.K. Culpepper, S.L. Bellis, The effect of collagen I mimetic peptides on mesenchymal stem cell adhesion and differentiation, and on bone formation at hydroxyapatite surfaces, Biomaterials 30 (10) (2009) 1898–1909.
- [61] N. Huettner, T.R. Dargaville, A. Forget, Discovering cell-adhesion peptides in tissue engineering: beyond RGD, Trends Biotechnol. 36 (4) (2018) 372–383.